



## **PROBABILISTIC SEISMIC HAZARD MAPS AT GROUND SURFACE IN JAPAN BASED ON SITE EFFECTS ESTIMATED FROM OBSERVED STRONG-MOTION RECORDS**

**Tadashi ANNAKA<sup>1</sup> and Yoshiaki OGANE<sup>2</sup>**

### **SUMMARY**

Site effect is very important for evaluating seismic hazard at ground surface. Deep soil structure as well as shallow soil structure affects site effect. Site and source effects on 5 % damped acceleration response spectra were simultaneously determined for a reference empirical attenuation equation by the regression analysis using the records obtained by dense observation networks in Japan. The distributions of site effects were represented by contour maps for spectral acceleration at representative periods. Using the obtained site effects we produced seismic hazard maps at ground surface for 1.0 sec and 0.2 sec spectral accelerations at return periods of 50 and 1000 years. The amplification characteristic of shallow soil structure is assumed to be linear for the seismic hazard maps. It will be necessary to take account of the strain dependence of dynamic soil properties individually for using the maps at a specified site.

### **INTRODUCTION**

Probabilistic seismic hazard analysis (PSHA) is a methodology for estimating the probability that specified levels of earthquake ground motions will be exceeded at a given location in a given future time period by combining the probabilistic models of earthquake occurrence and earthquake-caused ground motion. The result of the PSHA is represented as a seismic hazard curve for a specified site and as a seismic hazard map for a specified area. Although seismic hazard maps are usually given at the idealized common ground as the engineering base layer, it will be more preferable to be displayed as maps at ground surface for practical purpose.

Site effect is very important for evaluating seismic hazard at ground surface. Deep soil structure as well as shallow soil structure affects site effect. The Earthquake Research Committee of the Headquarters for Earthquake Research Promotion in Japan shows seismic hazard maps at ground surface using the amplification factor of peak ground velocity by shallow soil deposits determined based on micro-topography [1]. The approach of the amplification factor based on micro-topography is useful for the comparatively long-period index of ground motion as peak ground velocity. It is thought, however, that

---

<sup>1</sup> Engineering Seismologist, Tokyo Electric Power Services Co., LTD., Japan. Email: annaka@tepsc.co.jp

<sup>2</sup> Deputy Manager, The Tokio Marine Risk Consulting Co., Ltd., Japan. Email: y.oogane@tokiorisk.co.jp

the approach is not appropriate for the comparatively short-period index of strong motion as peak ground acceleration.

The approach for evaluating site effects more directly is based on the observed earthquake ground motion records at a site. Site effect can be conveniently and accurately determined as the deviations of the calculated acceleration spectra of observed records from those estimated by a reference empirical attenuation equation [2,3]. The effect of deep and shallow soil structure is included in the estimated site effects. It becomes possible to evaluate site effects in the Japanese whole country based on observed records by the deployment of Kyoshin Net (K-NET) [4] and Digital Strong-Motion Seismograph Network (KiK-NET) of the National Research Institute for Earth Science and Disaster Prevention of the Science and Technology Agency after the 1995 Hyogo-ken Nanbu (Kobe) earthquake.

The objectives of the present paper are to determine the site effects on 5 % damped acceleration response spectra using the records obtained by dense observation network in Japan and to display seismic hazard maps at ground surface using the estimated site effects

## EVALUTION OF SITE EFFECTS

### Data

The acceleration records obtained from the earthquakes with JMA magnitudes ( $M_j$ ) greater than or equal to 5.0 and with focal depths less than or equal to 200 km during the period from June 1996 to December 2002 by K-NET, KiK-NET, and the JMA-95 type accelerometer network of the Japan Meteorological Agency (JMA) were used. The records of a recent large earthquake, the  $M_j$  7.1 Miyagi-ken Oki earthquake of 26 May 2003, were added.

The data set consists of 24,655 pairs of orthogonal horizontal components from 251 earthquakes recorded at 1034 K-NET, 658 KiK-NET and 326 JMA stations. The records at ground surface were used at KiK-NET stations. Fault plane models for seventeen earthquakes with magnitudes approximately greater than 6.5 were compiled for determining shortest distance based on the previous researches, aftershock distribution and the results of teleseismic body-wave inversion analysis [5]. The other earthquakes are represented as point sources. The epicenter map of the 251 earthquakes and the location map of the 2018 sites are shown in Figure 1 and Figure 2, respectively. Data distribution for shortest distance and mean peak ground acceleration is shown in Figure 3.

### Method

Site effect can be determined as the geometrical average of the ratios of acceleration response spectra calculated from observed records to those estimated by a reference empirical attenuation equation [2]. Although this is a convenient method for evaluating site effect based on observed records, it is necessary to take account of source effect for determining site effect more accurately [3].

For evaluating site effects from the observed records an attenuation model for 5 % damped acceleration response spectrum proposed by Annaka et al. [6] was used as a reference empirical attenuation equation. The model is derived from the records of the JMA-87 type accelerometers obtained by JMA during the period from August 1988 to March 1996. The form of the attenuation equations is as follows.

$$\log SA(T) = Cm(T)M + Ch(T)H_c - Cd(T)\log(R + 0.334\exp(0.653M)) + Co(T) \quad (1)$$

Where  $T$  is natural period in sec,  $SA(T)$  is the mean spectral acceleration of two horizontal components for 5 % damped acceleration response spectra,  $M$  is JMA magnitude,  $H_c=H$  for  $H \leq 100\text{km}$  and  $H_c=100$  for  $100\text{km} < H < 200\text{km}$ ,  $H$  is the depth of the center of a fault plane of an earthquake in km, and  $R$  is the shortest distance in km to the fault plane. Common logarithms are used. The constants, 0.334 and 0.653,

are determined by the constraint that a peak ground acceleration becomes independent on magnitude when  $R$  reaches 0 km. The relations between regression coefficients and natural periods are shown in Figure 4. The constants,  $Co(T)$ , were determined so that the attenuation equation can be applied to a site whose subsurface S wave velocity is about 400 m/s.

In case of neglecting source effects, site correction coefficients of site  $j$ ,  $\beta_j(T)$ , is determined by the following Eq (2).

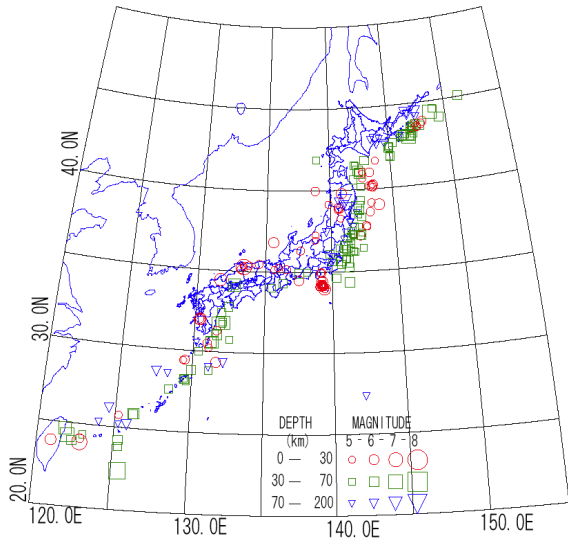


Figure 1: Epicenter map of earthquakes

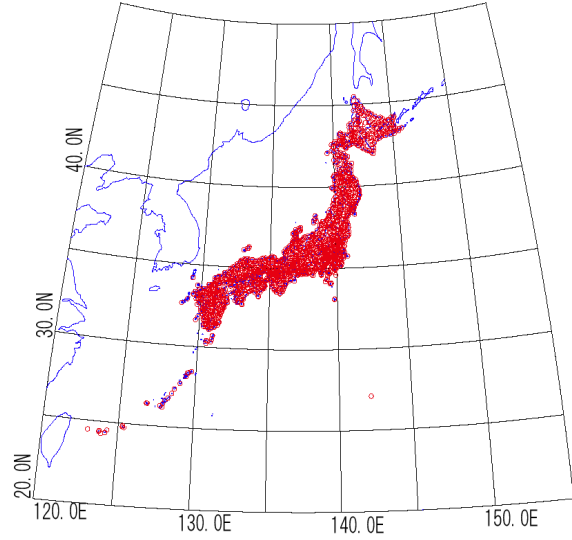


Figure 2: Location map of observation sites

$$\beta_j(T) = \frac{1}{n} \sum_{i=1}^n (\log(O_{ij}(T) / C_{ij}(T))) \quad (2)$$

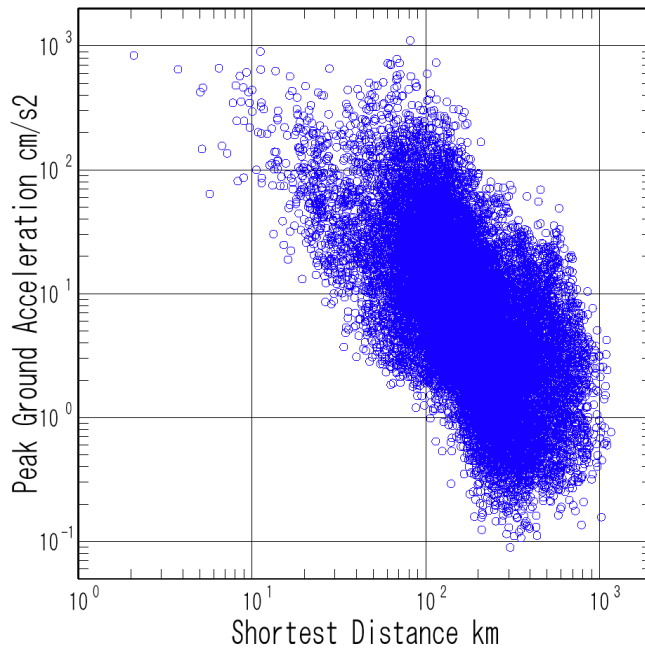


Figure 3: Distribution of shortest distance and peak ground acceleration

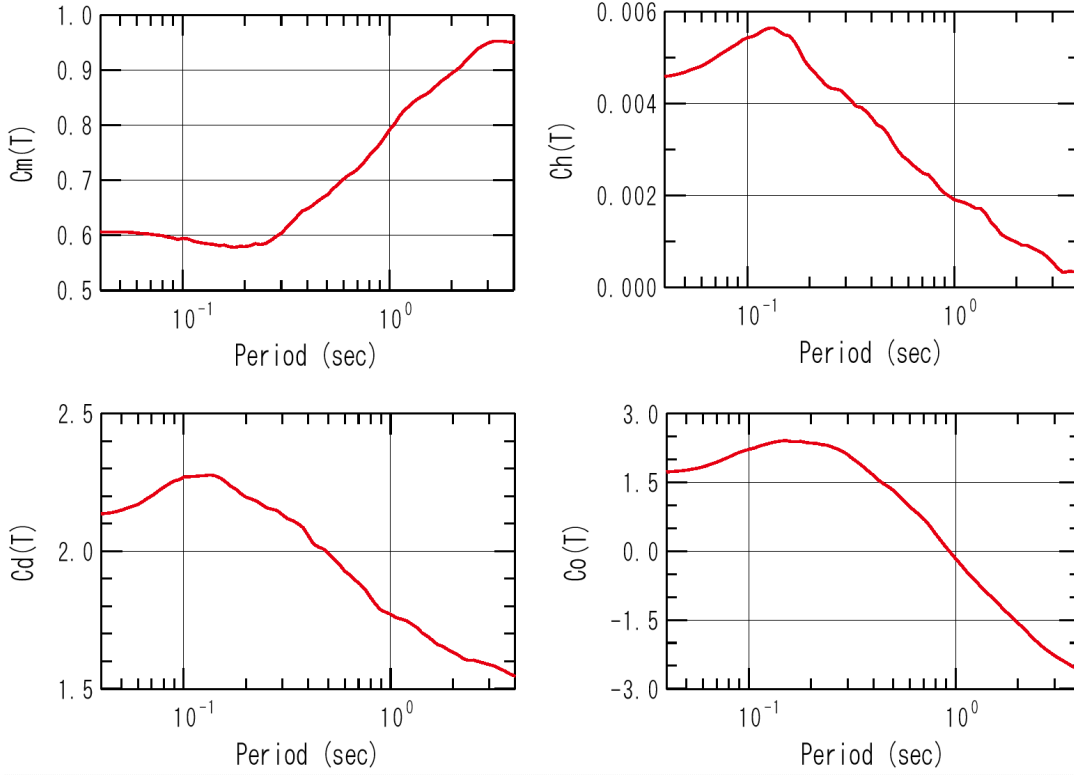


Figure 4: Relations between regression coefficients and natural periods

Where  $O_{ij}(T)$  and  $C_{ij}(T)$  are observed and calculated spectral accelerations for earthquake  $i$  and site  $j$ , respectively. The calculated spectral accelerations are estimated from the above empirical attenuation equation. We call this method 1.

In case of taking account of source effect simultaneously, the following Eq (3) is used instead of Eq (2).

$$\alpha_i(T) + \beta_j(T) = \log(O_{ij}(T)/C_{ij}(T)) \quad (3)$$

Where  $\alpha_i(T)$  are the source correction coefficients of earthquake  $i$ , and the others are the same as those in Eq (2). The regression equation, Eq (3), was solved by the least squares method using singular value decomposition. Constraint condition, Eq (4), is used.

$$\sum_{i=1}^{neq} \alpha_i(T) = 0 \quad (4)$$

The number of  $neq$  is the number of earthquakes used for constraint. We call this method 2.

## Results

The data with shortest distances less than or equal to 500 km were used in the analysis by taking account of the applicable distance range of the reference attenuation equation. The 179 earthquakes with observed sites greater than or equal to 20 were used for Eq (4). The site effects were evaluated by method 1 and method 2 for 1660 sites where the numbers of the observed earthquakes are greater than or equal to three and the source effects were evaluated for 250 earthquakes by method 2.

The site correction coefficients for the 1660 sites and the source correction coefficients for the 179 earthquakes by method 2 are shown in Figure 5 and Figure 6, respectively. For all range of periods, the

values of  $\beta(T)$  are distributed approximately from -0.7 to +0.9 and those of  $\alpha(T)$  are distributed approximately from -0.5 to +0.5.

The comparison of  $\beta(T)$  at the 1660 sites between methods 1 and 2 for the period of 1.0 sec is shown in Figure 7. The sites with large differences between the two methods are almost located in Ryukyu Islands and it may suggest that the separation of site and source effects is not good for this region. Except these sites, the differences are almost within  $\pm 0.1$ . The comparison of the distributions of the standard deviations in common logarithm for  $\beta(T)$  between method 1 and method 2 is shown in Figure 8. The data of the 479 sites with observed earthquakes greater than or equal to 15 were used. The standard deviations by method 2 are distributed around about 0.20 whereas those by method 1 are distributed around about 0.27. These results show that by taking account of source effects simultaneously, the standard deviations for  $\beta(T)$  decrease considerably but the values of  $\beta(T)$  are almost unchanged.

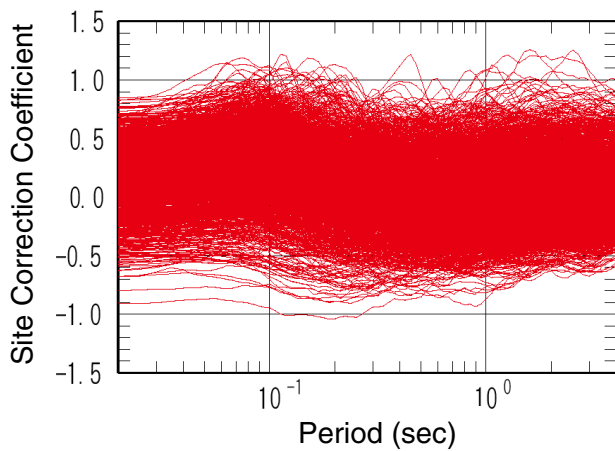


Figure 5: Distribution of  $\beta(T)$

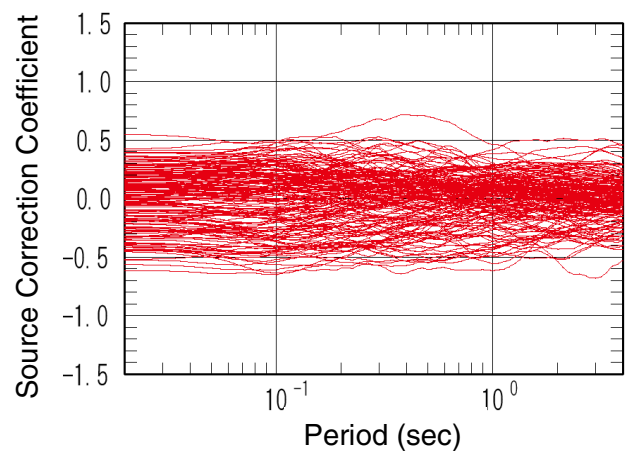


Figure 6: Distribution of  $\alpha(T)$

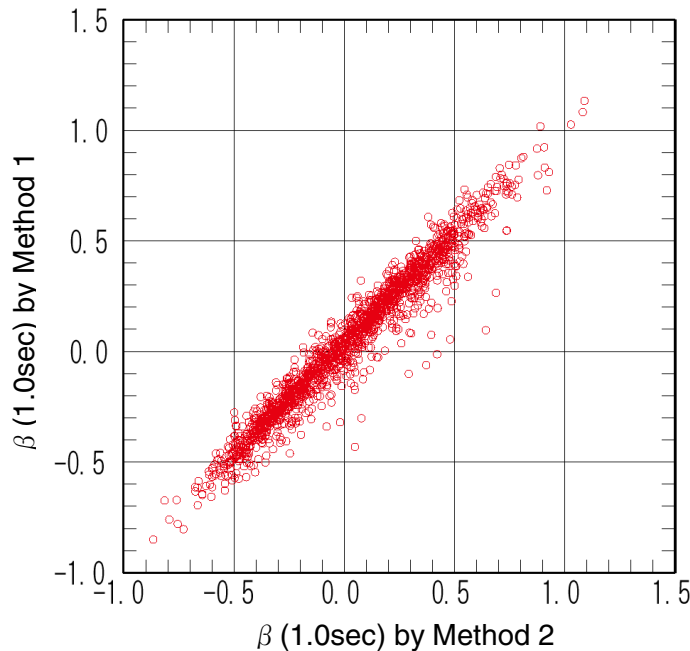


Figure 7: Comparison of  $\beta(1.0\text{sec})$  between Method 1 and Method 2

The geographical distributions of  $\beta(T)$  for the periods of 1.0 sec and 0.2 sec are shown in Figure 9 and Figure 10, respectively. The value of  $\beta(T)$  is represented by 10 symbols and the smoothed contours are drawn. The period of 1.0 sec is selected as the representative for longer-period range because the degree of earthquake damage is thought to be closely related to the intensity of spectral acceleration around 1.0 sec. The period of 0.2 sec is selected as the representative for shorter-period range because spectral acceleration usually becomes maximum level around 0.2 sec.

The distribution of  $\beta(T)$  for the period of 1.0 sec is clearly correspondent to the geographical features in Japan. The value of  $\beta(T)$  is high for the plain and basin districts whereas that is low for the mountainous districts. These tendencies can be seen all provinces in Figure 9. The distribution of  $\beta(T)$  for the period of 0.2 sec is significantly different from that for the period of 1.0 sec. For example, the tendency that the value of  $\beta(T)$  is high at the Pacific side and low at the Sea of Japan side can be seen in Hokkaido, Tohoku and Kanto. The high value districts of  $\beta(T)$  are located in the mountainous districts in Chubu, Kinki, and Chugoku. As a whole, it seems that the wavelength of the variation in  $\beta(T)$  at the period of 0.2 sec is shorter than that at the period of 1.0 sec. The difference between the periods of 1.0 sec and 0.2 sec may be attributed to that the site effects at the period of 1.0 sec are mainly controlled by deep soil structure whereas those at the period of 0.2 sec are controlled by both deep and shallow soil structure.

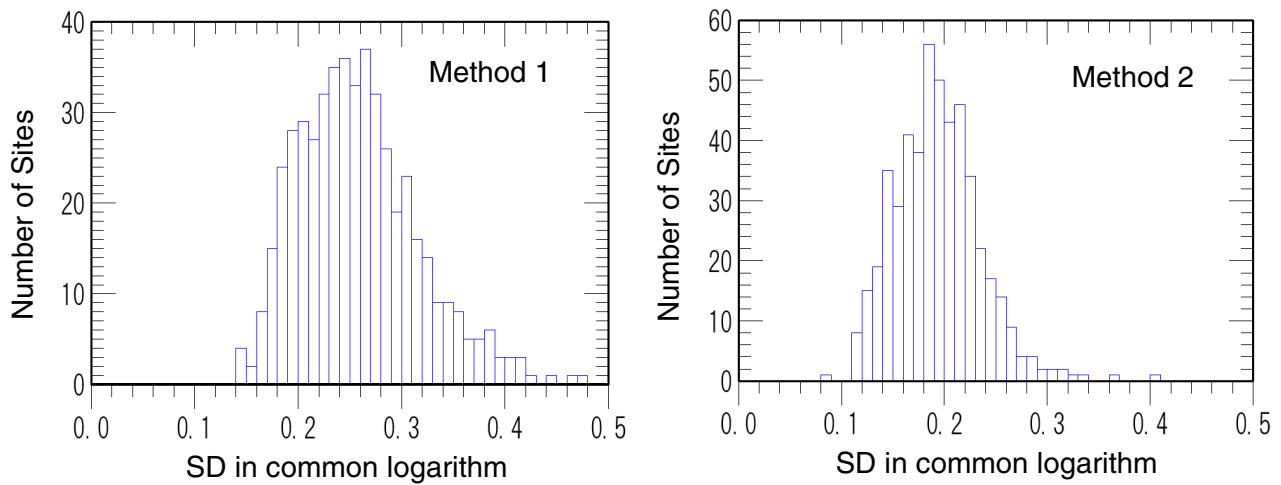


Figure 8: Comparison of distributions of SD for  $\beta$  (1.0sec) between Method 1 and Method 2

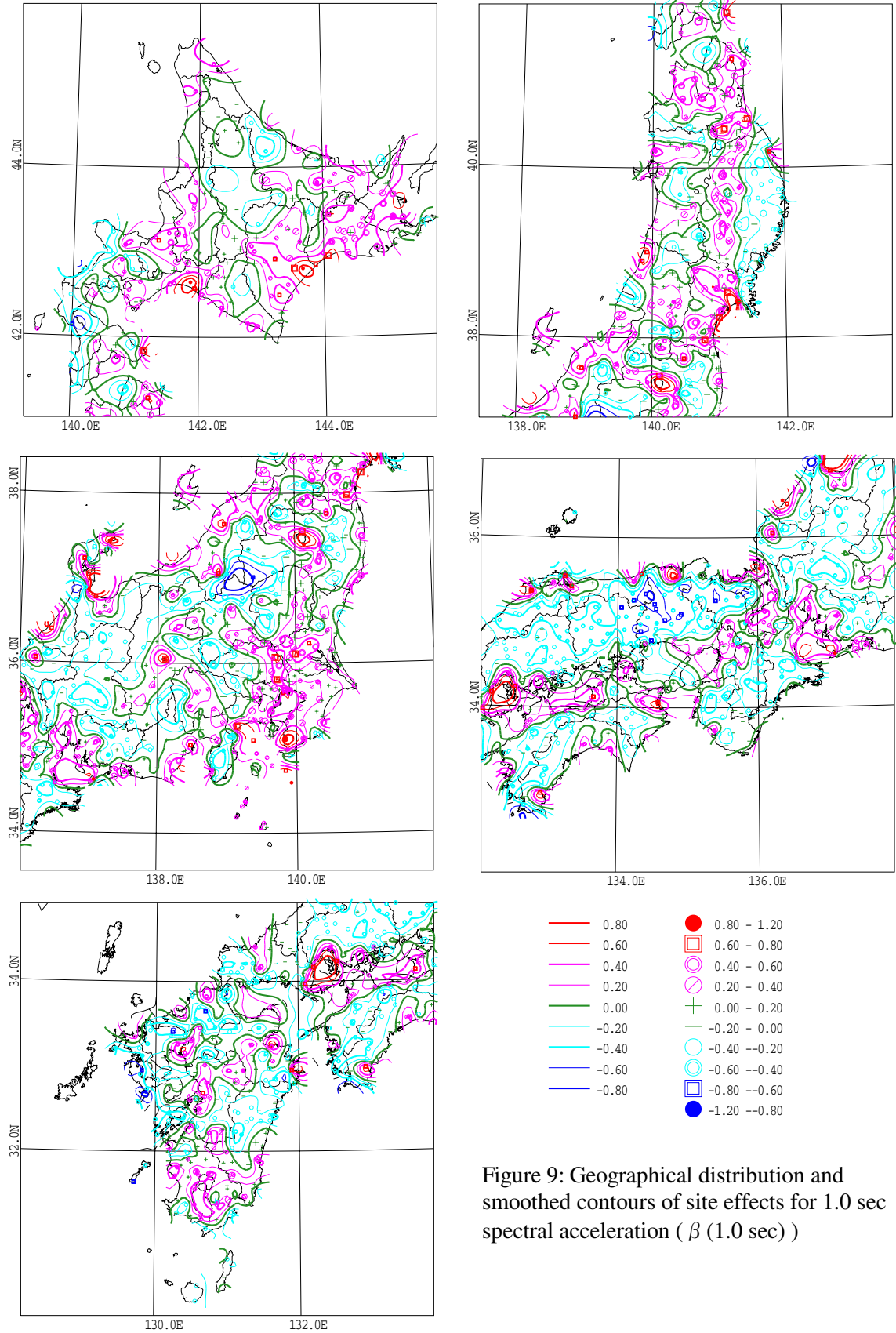


Figure 9: Geographical distribution and smoothed contours of site effects for 1.0 sec spectral acceleration ( $\beta$  (1.0 sec))

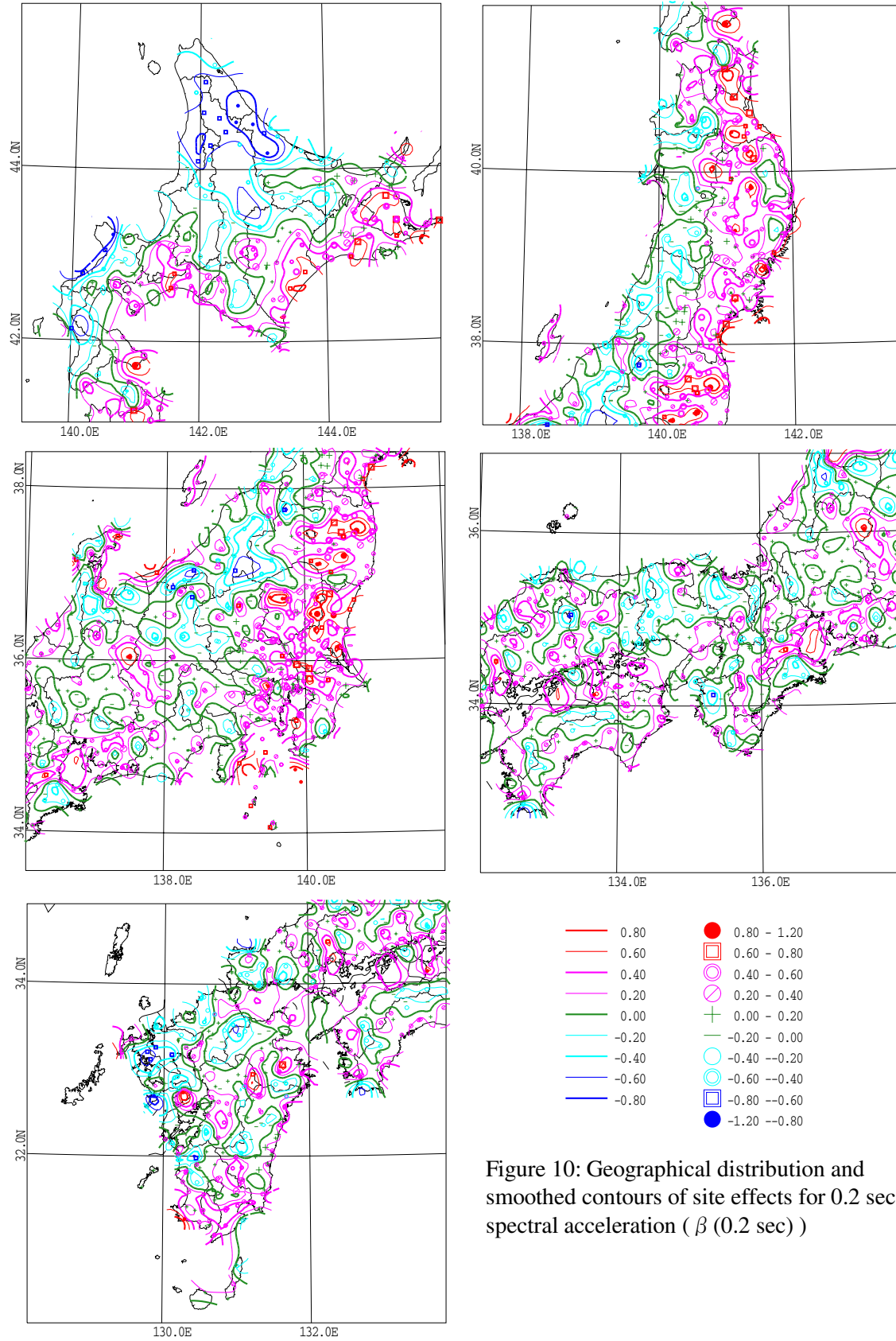


Figure 10: Geographical distribution and smoothed contours of site effects for 0.2 sec spectral acceleration ( $\beta(0.2 \text{ sec})$ )

## SEISMIC HAZARD MAPS AT GROUND SURFACE

### Earthquake occurrence model

The islands of Japan lie mainly on the Eurasia and Okhotsk plates. The Pacific and Philippine Sea plates subduct beneath the islands towards the west-northwest and northwest, respectively. The seismic activity in and around Japan is controlled by the interaction of the four plates.

For representing the seismic activity we used two types of seismic sources: (1) fault source generating large characteristic earthquakes, and (2) background seismic source generating small and moderate earthquakes. The earthquake occurrence model used in the present study is based on the model proposed by Annaka and Yashiro [7]. The model, however, was revised by taking account of the evaluation of active faults by the Earthquake Research Committee of the Headquarters for Earthquake Research Promotion in Japan [8].

The fault sources were defined based on the historical earthquake data and active fault data. Fault location and geometry, magnitude-frequency distribution, recurrence intervals (mean and variability) were determined for each fault source. Distribution of the fault sources of the revised model is shown in Figure 11. The major changes are the reflection of the evaluation on dip angle of fault plane for inland active faults and the widening of the application of the cascade model.

The background seismic sources were continuously defined along the upper plane of the Pacific plate, the lower plane of double planes of deep earthquakes in the Pacific plate, the upper plane of the Philippine Sea plate, and the seismogenic layer in the continental plates (the Eurasia and Okhotsk plates). Annual frequency of earthquakes with magnitudes greater than or equal to 5.0, b-value, and maximum magnitude were determined based on a truncated Gutenberg-Richter recurrence model for each background seismic source. The background seismic source model is the same as that of Annaka and Yashiro [7].

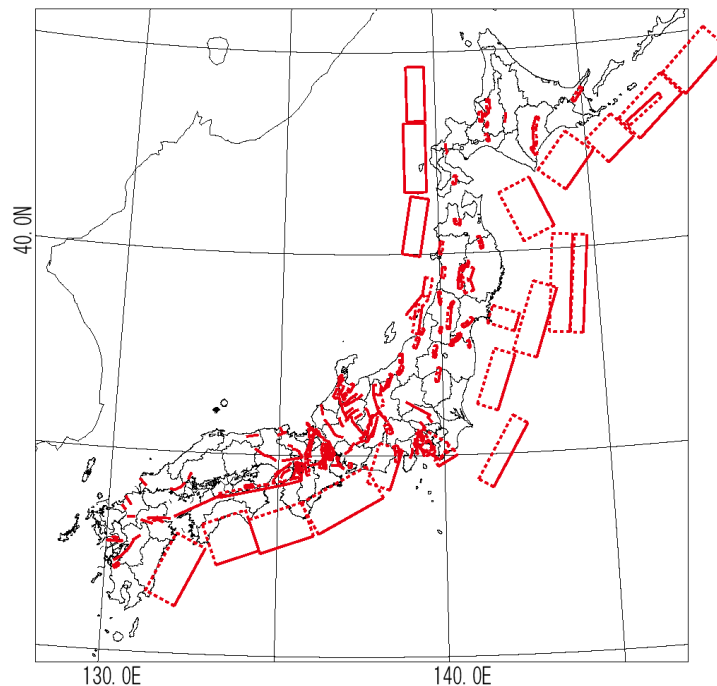


Figure 11: Distribution of fault sources (revised model)

### Seismic hazard maps at ground surface

The seismic hazard curves for 1.0 sec and 0.2 sec spectral accelerations were calculated for 1183 grid points in Japan except Ryukyu Islands using the estimated site effects from the observed earthquake ground motion records. The grid intervals for latitude direction and longitude direction are 10 minutes and 15 minutes, respectively. The earthquake occurrence model is assumed to be Poisson (average in long-term). The site correction coefficient for the reference attenuation equation at the center of each grid was determined by interpolation from the contours shown in Figures 9 and 10. The standard errors obtained at the regression of the reference attenuation equation [6] were used in common.

The seismic hazard maps at ground surface for 1.0 sec and 0.2 sec spectral accelerations at return periods of 50 and 1000 years are shown in Figure 12 and Figure 13, respectively. The site effects as well as the characteristics of seismicity have a strong influence on the seismic hazard maps. The return period of about 50 years is proposed for determining the earthquake ground motion for evaluating serviceability and the return period of about 1000 years is proposed for determining the earthquake ground motion for evaluating safety [9]. For 1.0 sec spectral acceleration, the median is about  $150\text{cm/s}^2$  at return period of 50 years and  $500\text{cm/s}^2$  at return period of 1000 years. For 0.2 sec spectral acceleration, the median is about  $400\text{cm/s}^2$  at return period of 50 years and  $1500\text{cm/s}^2$  at return period of 1000 years.

It is necessary to take notice that the amplification characteristic of shallow soil structure is assumed to be linear for the seismic hazard maps in Figures 12 and 13 because nearly all the observed records do not reflect the nonlinear effect of shallow soil structure. It will be necessary to take account of the strain dependence of dynamic soil properties individually for using the maps at a specified site. The process consists of three steps: modeling of shallow soil structure, deconvolution of the surface motion derived from seismic hazard maps to incidence motion at the base layer assuming the linear shallow soil structure, and estimation of surface motion from the incidence motion by nonlinear response analysis of the shallow soil structure.

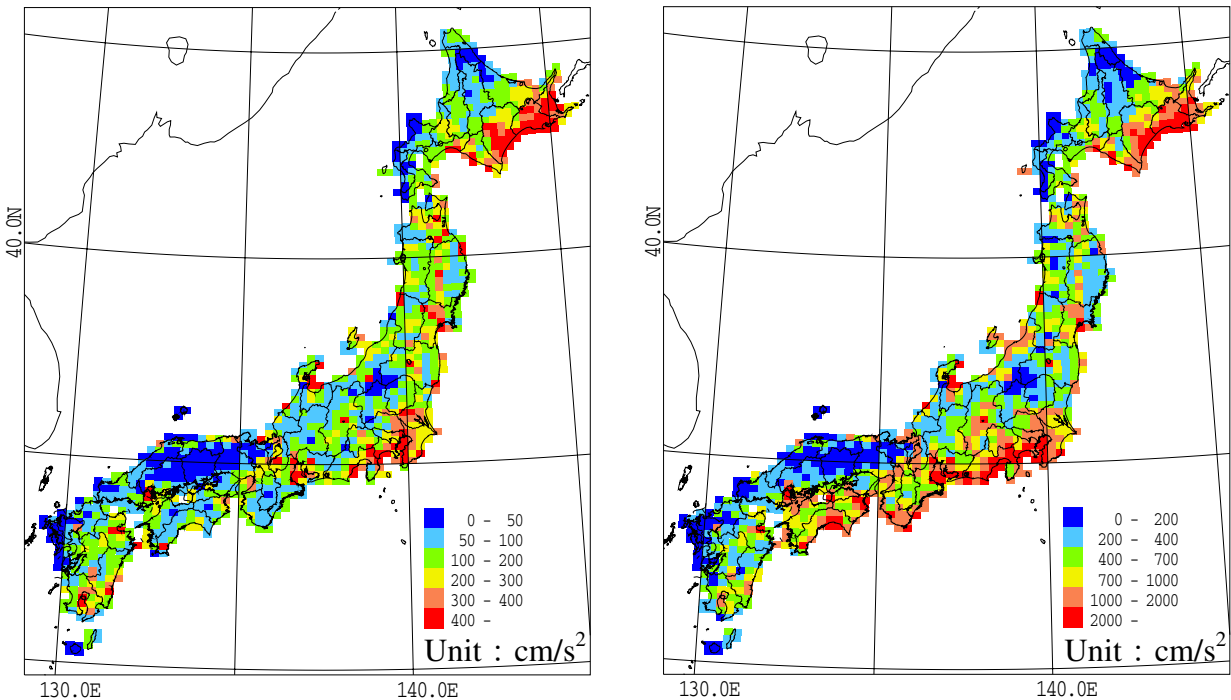


Figure 12: Seismic hazard maps for 1.0 sec spectral acceleration (Left: return period of 50 years, Right: return period of 1000 years)

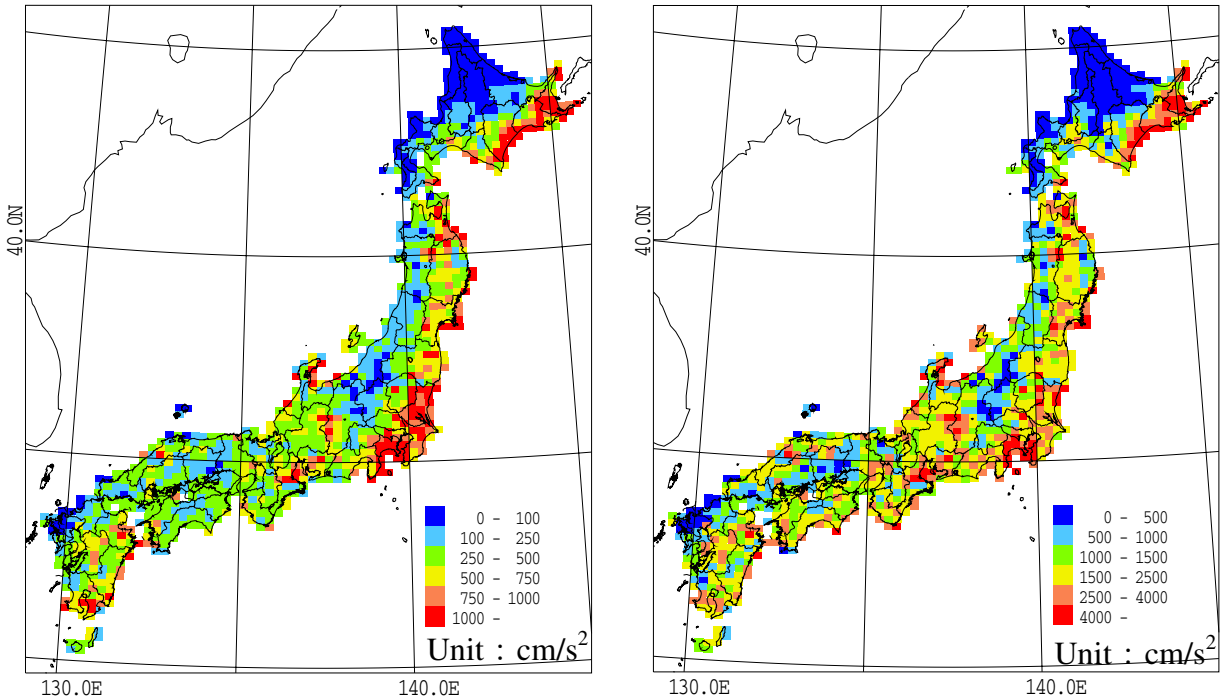


Figure 13: Seismic hazard maps for 0.2 sec spectral acceleration  
(Left: return period of 50 years, Right: return period of 1000 years)

## CONCLUSIONS

Site effects on 5 % damped acceleration response spectra were determined for a reference empirical attenuation equation by the regression analysis using the observed records obtained by dense observation networks in Japan. The results were represented by contour maps for spectral acceleration of representative periods. Using the obtained site effects we produced probabilistic seismic hazard maps at ground surface for 1.0 sec and 0.2 sec spectral acceleration at return periods of 50 and 1000 years.

Although we displayed the national contour maps of the site effects on acceleration response spectra in Japan for the first time in the present study, it will be necessary to examine the validity of the maps in more detail. Also it will be necessary to improve PSHA by taking account of the regional characteristics of source effects.

## ACKNOWLEDGMENTS

We thank the organizations that provided the earthquake ground motion data. We used the data by Kyoshin Net (K-NET) and Digital Strong-Motion Seismograph Network (KiK-NET) of the National Research Institute for Earth Science and Disaster Prevention of the Science and Technology Agency, and the JMA-95 type accelerometer network of the Japan Meteorological Agency.

## REFERENCES

1. Subcommittees for Long-term Evaluations and for Evaluations of Strong Ground Motion (2003): Preliminary version of probabilistic seismic hazard map (specific area: North Japan), <http://www.jishin.go.jp/main/index.html>.

2. Kurita, T., M. Kawahara, T. Annaka, and S. Takahashi (200): Evaluation of local site effects in the Kanto district based on observation records, Proceedings of 12th World Conference on Earthquake Engineering, Auckland, Paper No.224.
3. Annaka, T. (2002): Characteristics of the source and site effects on acceleration spectra in Japan, Proceedings of 12th European Conference on Earthquake Engineering, London, Paper no.187.
4. Kinoshita, S. (1998): Kyoshin-Net (K-NET), Seismological Research Letters, 69(4), 309-332.
5. EIC Seismological Note: [http://www.eic.eri.u-tokyo.ac.jp/EIC/EIC\\_News/index.html](http://www.eic.eri.u-tokyo.ac.jp/EIC/EIC_News/index.html).
6. Annaka T, Yamazaki F, Katahira F. (1997): A proposal of an attenuation model for peak ground motions and 5 % damped acceleration response spectra based on the JMA-87 type strong motion accelerograms, Proceedings of the 24<sup>th</sup> JSCE Earthquake Engineering Symposium, 161-164.
7. Annaka, T. and H. Yashiro (2000): Temporal dependence of seismic hazard in Japan Proceedings of 12th World Conference on Earthquake Engineering, Auckland, Paper No.316.
8. Earthquake Research Committee: Evaluation of active faults, <http://www.jishin.go.jp/main/index.html>.
9. Japan Society of Civil Engineers (2002): 2002 Enactment, Standard specifications for concrete structures, evaluation of seismic performance.